11176-6050-T000

PROGRAM VERIFICATION TEST RESULTS
LM/AGS FLIGHT PROGRAM NO. 6
(FORMERLY FPX)

May 1969

Prepared for:

National Aeronautics and Space Administration
Manned Spacecraft Center, Houston, Texas
Under Contract No. NAS 9-8166

Submitted by:

E.V. Avery

Approved by: for P.D. Joseph, Manager
System Design and Analysis
Department

Approved by: for H.B. Grossman, Manager
Data Processing Systems
Department

Approved by: T.W. Layton, Chairman
LM/AGS Software Design
Review Board

ACKNOWLEDGEMENT

The following individuals contributed significantly to Flight Program 6 verification.

E.E. Attala
E.V. Avery
T.S. Bettwy
B. Boyd
B. Burkett
R.L. Eshbaugh
D.M. Field
K.D. Freeman
M.J. Gunn
K. Kato
H.V. Kienberger
H.G. King
C.P. Lincoln
C.J. Mabee
F.B. Pettit
T.L. Rodrick
M.J. Ungar
T.C. Wilzbach
K.K. Wong

TABLE OF CONTENTS

1.0 INTRODUCTION

This report summarizes the results of the simulation testing of the LM/AGS Flight Program Number 6 (FP6). This program was formerly designated FPX. This testing was required to verify the program for the manned lunar landing (G) Mission. The simulation testing was done in accordance with the FP6 Verification Test Plan (Reference 1) as modified at the FACI (Reference 3). The verified flight program is designated LM/AGS FP6-S03 and is completely described in Reference (2).

The primary objectives of verification testing are to guarantee that the flight equations have been correctly implemented and as implemented perform acceptably.

1.1 Scope

Verification testing is the last in a series of equation and flight program testing leading to the verification of FP6. The testing which led to DMCP verification, FP3 verification and FP5 verification, was utilized here to support FP6 verification. By making use of DMCP, FP3 and FP5 testing, (see references 5, 6, and 7) FP6 testing could be concentrated in those areas where FP6 differed from these earlier programs.

This program verification process should not be confused with the system performance analysis, where the effect of all system errors on system performance is analyzed. In this document, performance refers to flight program (equation) performance and not system performance.

The verification testing results are partitioned into two parts:

- Section 5.0 contains a summary of the code check and Interpretive Computer Simulation (ICS) test results which were obtained from the FP6 checkout.
- Section 6.0 contains a summary of the Interpretive Computer Simulation/Flight Simulation (ICS/FS) and Scientific Flight Simulation (SFS) test results as well as the open loop ICS test results which were obtained from FP6 during verification.

1.2 Test Objectives

The primary objective of verification testing is to demonstrate that the changes to the AGS flight program 5 (FP5) through the incorporation of software change proposals (SCP's) 43, 50 and 51 are properly implemented to form the new FP6 program. Detailed test objectives for this sequence of tests are as follows:

(a) Demonstrate that FP6 is equivalent to FP5 which has been verified for the lunar mission, except for those changes in operational capability implemented in accordance with the approved SCP's.

(b) Demonstrate that the software changes are correctly implemented in FP6 and as implemented meet the mission software requirements.

(c) Determine equation performance in those flight equation areas affected by the software changes.

(d) Demonstrate the functional capability of the program on a lunar landing type mission.

1.3 Test Concepts

The flight program is tested by inserting it into an Interpretive Computer Simulation (ICS) which simulates the flight computer in detail. The detail of this computer simulation is such that flight computer and ICS outputs are identical when subjected to identical inputs and when both computer and ICS contain the same flight program. Some functions in the flight program are tested by programming drivers to supply inputs to the ICS. This is referred to as ICS testing in this report.

Flight program functions such as guidance and steering are best tested in a flight simulation where the guidance, control system and dynamics closed loop is simulated. This simulation, where an ICS and Flight Simulation (FS) are integrated, is designated an ICS/FS, and this testing is referred to as ICS/FS testing. A detailed description of the ICS/FS is presented in Reference (9).

The mission for any ICS/FS test case is determined prior to the run. Astronaut or PGNCS discretes are entered via a function table as a function of time. Several astronaut actions are simulated by monitoring flight program quantities. For example, the TPI burn may be initiated when θ_{LOS} as displayed via DEDA reaches a desired value.

ICS/FS test results involving the actual LM state during the test cases are obtained directly from the flight simulation. Test results concerning flight program performance are obtained by comparing flight program quantities with the actual quantities as obtained from the flight simulation. Additional test results which determine flight program coding and flight computer word size effects on total flight program performance are obtained by comparing ICS/FS results with the results of scientific (engineering) flight simulations.

Deliberately large initial conditions and perturbations are simulated to check that no scaling and timing problems exist throughout the regions of expected operation. Checks are made to assume that no unexpected overflows or timing problems occur.

ICS test results are evaluated by comparing flight program quantities with precomputed reference or desired values or with scientific simulation results.

1.4 Test Criteria

The test criteria were selected to demonstrate satisfactory implementation of the flight equations in FP6. The results of these verification tests determine the flight equation performance and flight computer quantization errors, and are not indicative of total AGS performance which includes the effects of sensor errors, initialization errors, etc.

Reference (4) states for the lunar landing mission that during the period from initiation of powered descent to the completion of orbit insertion after an abort from hover, the navigation computation error accumulated in each component of LM inertial position and velocity shall be less than the following:

(a) 2500 ft in x, y and z (inertial position)

(b) 4 fps in x, y and z (inertial velocity)

This requirement was demonstrated in the DMCP testing, Reference (7), and since the navigation equations in FP6 and DMCP are identical, this requirement is considered satisfied.

Some test cases are identical or almost identical to previous cases run with the FP5 program prior to the software changes. The test criteria here is that the test case results be essentially identical to the results given in Reference (5).

All but one of the ICS/FS test cases were also run using the SFS. The test criteria here is that the results of both simulations have reasonable agreement.

Read and pass on Tyer!

2.0 SUMMARY

The AGS Flight Program deck designated LM/AGS FPX-S03 0151 dated 2-14-69 has been verified according to the test plan of Reference (1). With the exception of the discrepancy described in Section 2.1, the required changes have been incorporated correctly and the desired results achieved. Of particular significance is the fact that the flight program has been shown to have scaling consistent with the currently proposed G Mission (Reference 8) and operates as follows:

(a) The newly programmed CSI/CDH equations have been shown to function correctly and without unexpected overflows for both the case where CDH occurs 1/2 orbital period and 3/2 orbital periods following CSI.

(b) The newly programmed orbit insertion equations have been shown to operate correctly and without unexpected overflows.

(c) The newly programmed radar filter has been shown to operate correctly and without unexpected overflows.

(d) All areas of the program unchanged from FP5 have been shown to be unchanged.

2.1 Discrepancy Affecting One DEDA Display and Four Telemetry Quantities

As a result of the program verification testing, a minor discrepancy was discovered that in no way compromises flight program performance. When the CDH routine is in use, the DEDA displayed and telemetered magnitude of the velocity-to-be-gained may not be correct. In addition, the telemetered components of the inertial vector velocity-to-be-gained and the corresponding components of the desired pointing direction for the thrust axis ($\underline{X}_{bD}$) may be invalid when either the CSI or CDH routine is in use. However, once the External ΔV guidance mode has been selected, which is the required procedure for the execution of the AGS controlled CSI and CDH maneuvers, the same DEDA display quantities and telemetered quantities will be correct. As a consequence of the existing program coding, the system operator must switch to the External ΔV mode when monitoring of the affected quantities via DEDA or telemetry is desired.

The discrepancy involved occurs in the computer transformation given in equation (2.1)

$$\underline{V}_{GI}\ (t_{ig}) = [T]\ \underline{V}_{GLV}\ (t_{ig}) \tag{2.1}$$

where t_{ig} = time of the maneuver

$\underline{V}_G\ (t_{ig})$ = velocity-to-be-gained vector at time of maneuver.

subscript I means components of vector in inertial coordinate system

subscript LV means components of vector in local vertical coordinate system.

It was intended that when the AGS is in the CSI or CDH mode the matrix $[T]$ be computed as given in equation (2.2)

$$[T] = [\underline{U}_1\ (t_{ig}),\ \underline{V}_1\ (t_{ig}),\ \underline{W}_1\ (t_{ig})] \tag{2.2}$$

where $\underline{U}_1$ = normalized LM position vector

$\underline{V}_1$ = unit vector directed downrange from the LM and parallel to the CSM orbit plane

$\underline{W}_1$ = Unit vector given by the equation $\underline{W}_1 = \underline{U}_1 \times \underline{V}_1$

However, the vector $\underline{V}_1\ (t_{ig})$ was not saved and the actual computer mechanization when the AGS is in the CSI or CDH mode is equation (2.3).

$$[T] = [\underline{U}_1\ (t_{ig}),\ \underline{V}_1\ (t),\ \underline{W}_1\ (t_{ig})] \tag{2.3}$$

where t represents the present time.

The result of using $\underline{V}_1\ (t)$ rather than $\underline{V}_1\ (t_{ig})$ is an incorrect transformation when the computer is in the CSI or CDH mode. This means that when the desired thrust vector pointing direction $\underline{X}_{bD}$ is computed by the equation (2.4)

$$\underline{X}_{bD} = \frac{\underline{V}_{GI}}{|\underline{V}_{GI}|} \tag{2.4}$$

the wrong result is achieved. Likewise, the magnitude of the vector will be incorrect. When the computer is in the CSI mode, however, the local vertical component of the velocity-to-be-gained is zero resulting in a $\underline{V}_{GI}$ vector with the correct magnitude but the wrong direction. Note that as $t \rightarrow t_{ig}$ the transformation (2.1) becomes correct.

When the computer is in the External ΔV guidance mode the matrix [T] is computed based on the present time

$$[T] = [\underline{U}_1 (t), \underline{V}_1 (t), \underline{W}_1 (t)] \tag{2.5}$$

This is an ortho-normal transformation and hence equation (2.1) is correct.

3.0 MODIFICATIONS TO THE TEST PLAN

Some additions and modifications to the test cases as specified in the FP6 program verification test plan were made to give further insight into program performance. These are described below.

Group 1 ICS/FS Test Cases

Case 1.3 of the original test plan was modified so that the initial conditions corresponded to those which exist at CSI time for the nominal G-Mission of Reference 8. This change also affected case 1.14 which used the same initial conditions as case 1.3 except for the addition of simulated navigation errors.

Group 2 Open Loop ICS Test Cases

In addition to the 3σ radar filter cases called for by the test plan, numerous other test cases were run which included many noise-free and noisy nominal and 10σ perturbed initial condition cases.

An additional series of 23 CSI cases and 6 CDH cases consisting of highly perturbed vehicle states and target conditions were run in an open loop manner in the ICS.

Group 3 SFS Test Cases

Due to the change in ascent abort targeting, some of the test plan cases were changed or eliminated.

Case 3.1 was changed to a liftoff from the lunar surface with an initial LM position 2 degrees out of the CSM plane. This case was designed to verify AGS out-of-plane steering capability with updated yaw jerk-limiting constants.

Cases 3.2, 3.11 and 3.12 were eliminated, since α_L will be limited to a fixed value by lunar surface retargeting.

Case 3.10 was changed to a nominal abort from the lunar surface since no reference ascent trajectory was available except AGS generated lunar surface aborts.

Case 3.5 and the SFS version of case 1.11 are orbit insertion burns that were performed 2 ways:

1) 100% DPS throttle until orbit insertion
2) 100% DPS throttle until $\dot{h} > 0$, then 50% DPS throttle until orbit insertion.

4.0 TEST SET UP

The three simulations used for FP6 verification were the Interpretive Computer Simulation (ICS), the Interpretive Computer Simulation/Flight Simulation (ICS/FS) and the Scientific Flight Simulation (SFS). Each of these consisted of a controlled deck or decks of cards which were input to the IBM 7094 computer to obtain each simulation case. A listing of selected quantities plus a set of plots of selected quantities were made by a printer or Cal-Comp plotter to display the data from each case.

The Performance Analysis program was used to generate the required input quantities for the group 2 open loop ICS radar filter test.

4.1 ICS/FS Configuration Control

Configuration control of the ICS/FS consisted of controlling the functional configuration of the 5 decks comprising the ICS/FS. Control of each deck was ensured by listing the compressed deck identification on each ICS/FS run listing. A new compressed deck would have a new identification.

The five compressed decks used during FP6 verification were identified as follows:

ICS Deck: ICS-C dated 11-6-68
N-Stage Deck: NS Prog. - B dated 3-7-68
Interface Deck: INTERFACE - C dated 2-15-69
N-Stage Data Deck: LUNAR MILESTONE - E dated 2-13-69
Flight program: LM AGS FPX-S03 0151 dated 2-14-69

5.0 FP6 Program Checkout Results

5.1 Introduction

The objective of the program checkout testing was to demonstrate that the flight equations had been correctly coded and implemented into LM/AGS Flight Program 6 (FP6). Those functions tested during checkout testing of previously verified flight programs were rechecked to the extent necessary to ensure their correct functioning. This category includes such computations as navigation and direction cosine updating and TPI guidance solutions.

All computations introduced by software changes were compared to appropriate scientific simulation computations and hand-checked. A timing study of all program logic branches was performed. The output telemetry list was reviewed for correct definitions and time applicability.

5.2 Preliminary Code Check Procedures

The checks and tests described in this section verified that the coding of the equations had been successfully accomplished. The checks and tests fell into two groups. The first consisted of a study of the program itself, including an analysis of the instructions, constants, and erasable memory. The second group involved making limited duration open-loop interpretive routine runs, some with temporary control logic modifications, in order to evaluate the performance of individual segments of the program.

FP6 was first assembled from an early version of FP5 which was identical to Flight Program 3, Revision A (deck ID=0005) with the exception that all computer variables which contained a length dimension in their units were scaled for lunar ranges. Then, software changes 41, 42, 44, 45, 46, 48 and 49 were incorporated into FP6 in parallel with FP5. Also, the software changes 43, 50, and 51 - revised radar filter, CSI, CDH, and orbit insertion solutions - were incorporated into FP6.

Checkout began with an assembly program compilation of the final version of the FP6 program. The assembly program included checks for duplicate and unassigned symbols, constants outside scaling limits, and illegal instructions. It produced a listing and a punched deck which corresponded to the assembled program. The assembled listing was checked for consistency with the desired program by reviewing the comments field, particularly for scale factor information.

A symbol reference table, obtained with the program listing, was used to identify all symbols with the equations referencing them. This ensured proper assignment of memory storage and connection between program routines.

A listing of the program constants was generated, and checked for satisfactory agreement between input values and computer scaled values. A set of flow charts was prepared, and the flow charts and program constants listing were submitted for internal review and concurrence.

5.3 Summary of FP6 Simulations and Checks

5.3.1 Miscellaneous Checks

A timing study of the FP6 program was performed. Worst-case timings of all logic paths in the 20-msec, 40-msec, and 2-sec computations were hand computed using the program listing. These timings were verified by utilizing the trace features of the ICS program. Using the results of this study, the 2-sec computations were partitioned into suitable branches.

Constants and variables were checked to ensure that each has a binary scaling consistent with its range and desired accuracy. All time-shared and mode-shared quantities were checked to ensure that such sharing is consistent with the usage of each quantity. Quantities used for entry or readout via DEDA were placed in the correct decimal or octal DEDA scale factor regions of the scratchpad memory. Two new DEDA decimal unit conversions, providing accelerometer bias compensations in units of ft/sec^2 and the ullage counter constant, 1K9, in units of 2-sec counts, were added.

A simulation was run to check DEDA input and output capabilities. Scale factor accuracy and correct scale factor selection were tested by inputting to or outputting from every memory address which is at a scale factor boundary. Also, an attempt to input data into DEDA protected regions (SCP 44) verified correct implementation of the protection.

The DEDA immediate action entries, AGS absolute time and radar update signal S_{15}, were tested, and the resulting computations were hand-checked.

The BTME tape load checksum routine, modified to sum all memory locations from 0206_8 to 3777_8, was tested. Following the checksum computation, the program startup routine was executed, and all affected quantities were observed to be correctly computed. Then simulated gyro and accelerometer inputs, chosen to cycle the direction cosine scaling selection logic from low rate to high rate and back to low rate, were input. All direction cosine quantities compared exactly with those of an identical FP3 direction cosine test case.

A downlink initialization was performed. The routine was tested with an invalid ID word. Then, the proper ID word and state vectors were input. All computations were hand-checked. Following the state vector updates, the altitude, altitude rate, and out-of-plane velocity V_{y0} (SCP 45) were compared to the altitude, altitude rate, and lateral velocity register outputs, respectively. (Each quantity was less than the full-scale value of its meter.) The new altitude scale factor (least significant bit = 2.345 feet) was checked.

LM and CSM state vector initializations were correctly performed, after which the correct limiting of the altitude and lateral velocity register outputs was observed.

A body axis align was performed, and all direction cosine quantities were properly computed. The FDAI register outputs were then hand-checked. A PGNCS/AGS align, using Euler angles (45°, 90°, 315°), was correctly performed (SCP 41), and S_{00} was automatically reset to zero. The FDAI outputs were again checked.

During each guidance mode, a 2-sec sampling of 100 output telemetry words was checked. Each word was correct and had time applicability consistent with the flow charts. The telemetry initialize routine and the combining of S_{12} and μ_8 into one telemetry word were checked.

A simulation was performed to test the direction cosine scaling selection logic when the changeover value of the low/high rate logic was simulated on one gyro axis and the other two gyro inputs were zero. A DEDA entry into S_{13} was performed to check the computations of $\sin\delta_L$ and $\cos\delta_L$ and the setting of the lunar surface flag.

5.3.2 Attitude Errors and Engine Discretes Logic

Several simulations were performed to exercise every path in the 40-msec attitude errors computation logic and engine discretes logic. Correct logic path selection was tested using the trace features of the ICS. Attitude error register outputs were compared to hand computations.

5.3.3 Orbit Insertion Guidance Routine

The orbit insertion simulation was initialized to duplicate a scientific simulation. A constant acceleration was input to the X-axis accelerometer; all other ASA inputs were zero. Initially, the LM altitude and altitude rate were less than the safe values of 21J and 22J, and $\underline{X}_{bD}$ and V_G were correctly computed for vertical steering. Then, when $\dot{r}$ exceeded 22J, correct steering computations were again observed.

At several times during the case, each orbit insertion solution quantity was compared to the scientific simulation value or hand-computed value. Also, LM positions and velocities were compared every 2 sec.

All logic paths of the $\ddot{r}_d$ lower limit computation (SCP 46) were exercised. An altitude update via DEDA (SCP 42) was performed.

A self-test checksum failure was forced, and S_{12} and the test mode failure discrete were properly set. The combined self-test and ullage counter word for telemetry was checked.

5.3.4 CSI, CDH, and External ΔV Guidance Routines

Five CSI and CDH simulations were performed and compared to scientific simulation cases 1.0 (S_{16}=1), 6.2 (S_{16}=3), 1.24 (S_{16}=1), 7.4 (S_{16}=1), and 6.9 (S_{16}=3).

The outline of each case is as follows:

The case was initialized eight seconds prior to the time of the CSI maneuver with S_{10}=1. LM and CSM positions and velocities and all CSI solution quantities were compared to scientific simulation values or hand computations for $t < t_{ig}$, $t = t_{ig}$, and $t > t_{ig}$. When t exceeded t_{ig}, T_{Δ} was correctly limited to zero.
The external ΔV mode was then selected via DEDA and observed to have been automatically targeted for performing the CSI burn.

Then, the state vectors were updated to be valid eight seconds before the time of the CDH maneuver, and the CDH guidance mode was selected via DEDA. CDH solution quantities, external ΔV targeting, and navigation were checked prior to, at, and after time t_{ig}, as in the CSI mode.

The external ΔV mode was then selected via DEDA and observed to have been automatically targeted for performing the CDH burn.

Self-test was successfully passed in four of the simulations and forced to fail in the fifth case.

5.3.5 TPI and External ΔV Guidance Routines

This simulation duplicated the FP5 TPI checkout case. LM and CSM navigation, time to perigee, apofocus and perifocus altitudes, and the angle ξ (SCP 49) compared exactly between the two runs.

The simulation began in the TPI search mode (S_{10}=3) with J^6=2880 sec and J^4=1095 sec. All TPI solution quantities and external ΔV maneuver computations (SCP 48) were correct. The TPI execute mode was selected, and solutions were again compared. J^4 was set equal to J^6 via DEDA, and the logic path which zeroes J^4 was exercised. V_T was set equal to K_{11}^2 for two seconds, after which a valid TPI solution with J^4=0 was computed.

J^6 was set equal to zero via DEDA to exercise the TPI logic for invalid time targeting. Then, J^6 was set to 2880 sec, and the external ΔV routine was entered. **It was observed that the external ΔV mode had been automatically targeted for performing the TPI burn.**

An accelerometer calibration was commanded by setting S_{00} to 7 via DEDA. After 32 seconds of calibration, S_{00} was set to 6 via DEDA to initiate a gyro and accelerometer calibration. As a result of this entry, the calibration counter was zeroed and an automatic PGNCS/AGS align was performed, followed by the calibration.

5.3.6 External ΔV Guidance Routine

In order to check this routine an axis-by-axis burn, with no automatic steering, was simulated. The sequence of events and the resulting AGS response which was checked is listed below.

Event	Results
S_{10} set = 5	
External ΔV velocity-to-be-gained components entered (1 fps, 2 fps, -1 fps)	Correct maneuver targeting for External ΔV mode observed
X-body-axis thrusting simulated	Ullage counter incremented, S_{07} set automatically = 1
	X_{bD} vector frozen since $V_G < 15$ fps X-body-axis velocity-to-be-gained decremented
X-body-axis thrusting off	Ullage counter reset
Y-body-axis thrusting simulated	Y-body-axis velocity-to-be-gained decremented
Z-body-axis thrusting simulated	Z-body-axis velocity-to-be-gained decremented
	At completion of simulated thrusting, all velocity-to-be-gained vectors = 0
TPI mode entered	S_{07} set = 0
	Accumulated sensed velocity vector $\Delta\bar{q}_s$ set = 0
External ΔV mode re-entered	External ΔV mode had been automatically targeted for performing the TPI burn.
	Self test successfully passed for this simulation

5.3.7 Radar Filter Routine

The radar filter was checked by introducing initial errors into the LM state vector, and then making range and range rate updates over a period of 1320 seconds. To simplify the comparison of results to other simulations, those quantities saved following a DEDA entry into S_{15}: Z-body direction cosines, the computed range vector and range rate, and time between radar range inputs were input directly. These quantities were entered at the times labeled with Z on the timeline. The initial in-plane error magnitudes were 30,000 feet in both x and y coordinates and 30 fps in V_x and V_z.

The initial out-of-plane error magnitudes were 45,000 feet in the y coordinate and 45 fps in V_y. Radar measurements contained no noise.

The measurements schedule used for the range and range rate updates was as shown in the following diagram.

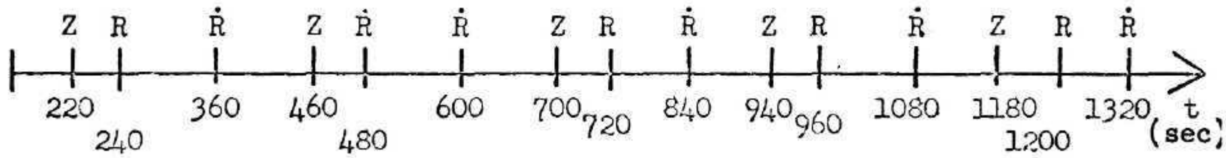

The checkout test runs showed that initial condition errors in position and velocity were reduced by increasing the number of radar data points. For this radar measurement schedule, both estimated state errors and the covariance matrix had reached steady-state at the end of radar measurements.
Radar filter verification test results will be disscused in Section 6.

All quantities were hand-checked at several times during the simulation. Hand computations were performed to include AEA quantization and rounding, and exact bit-for-bit comparisons were achieved for range rate update quantities.

Covariance matrix propagation portions of the radar filter (i.e., filter without range or range rate inputs) yielded bit-by-bit comparison with earlier ICS runs made during radar filter development.

S_{17} was set to 1, and correct filter initialization was observed.

6.0 PROGRAM VERIFICATION RESULTS

The FP6 verification results are summarized in three parts. Group 1 consists of program verification cases which include the ICS/FS runs, called out in FPX Verification Test Plan (Reference (1)) and the SFS runs that duplicates the maneuver performed in the respective ICS/FS case.

Group 2 consists of open loop ICS runs and Group 3 consists of SFS runs.

The numbers used to identify each case correspond directly with the number in the test plan (Reference 1).

Table 6.1 summarizes the verification test cases which were run.

6.1 Group 1 - ICS/FS Test Case Results

The ICS/FS test cases may be separated into three classes as follows: (1) cases which were a repeat of a similar FP5 test case, (2) cases which were based on conditions in the G-Mission, and (3) cases which were designed to test particular software changes which require conditions which would not be encountered in the nominal G Mission.

The following pages describe each case, its objectives, and the conclusions.

Table 6.1

Earl Avery ICS/FS

FP6 Verification Test Cases

Type Lisa Freeman Scientific

ICS	ICS/FS	SFS	P.A.*	Case Number	Description
	X			1.1	Lunar surface landing
	X	X		1.2	Lunar surface abort
	X	X		1.3	CSI burn with CDH 1/2 LM orbital period after CSI
X	X	X		1.4	CSI ~~CDH~~ burn with CDH 3/2 LM orbital period after CSI
	X	X		1.5	CDH burn using external ΔV pad load
	X	X		1.6	CDH burn with removal of out-of-CSM plane component of LM velocity
	X	X		1.7	TPI and first midcourse burn
	X	X		1.8	TPI burn with Z-axis RCS engines
	X	X		1.9	Abort at 2000 feet altitude
	X	X		1.10	Multiple guidance solutions during coast phase
	X	X		1.11	Abort from perturbed descent trajectory a) 50% Trust b) 100% Trust
	X	X		1.12	Abort late in powered ascent
	X	X		1.13	Pre TPI radar filter test
	X	X		1.14	Pre CSI radar filter test
X			X	2.1	Pre-CSI 3σ radar filter test (Schedule 1)**
X			X	2.2	Pre-CDH 3σ radar filter test (Schedule 1)
X			X	2.3	Pre-TPI 3σ radar filter test (Schedule 1)
X			X	2.4	Post-TPI 3σ radar filter test (Schedule 1)
X			X	2.5-2.8	Same as 2.1-2.4 except with Schedule 2
X			X	2.9-2.12	Same as 2.1-2.4 except with Schedule 3
X			X	2.13	Pre-CSI nominal radar filter test (Schedules 1 and 4)
X			X	2.14	Pre-CDH nominal radar filter test (Schedules 1 and 4)
X			X	2.15	Pre-TPI nominal radar filter test (Schedules 1 and 4)
X			X	2.16	Post-TPI nominal radar filter test (Schedules 1 and 4)
X			X	2.17-2.20	Same as 2.12-2.15 except with 10σ perturbed initial conditions
		X		3.1	Liftoff from lunar surface with 2 degree wedge angle
		X		3.3	Out-of-plane CSI burn with positive state vector perturbations
		X		3.4	Out-of-plane CSI burn with negative state vector perturbations
		X		3.5	Abort 100 seconds into powered descent
		X		3.6	Abort 200 seconds into powered descent
		X		3.7	Abort 350 seconds into powered descent
		X		3.8	Abort 500 seconds into powered descent
		X		3.9	Abort at hover
		X		3.10	Nominal abort from surface
		X		3.13	Abort 150 seconds into powered descent with positive state vector perturbations
		X		3.14	Abort 150 seconds into powered descent with negative state vector perturbations
		X		3.15	Abort in powered ascent 10 seconds before expected insertion
X		X		3.16	Direct intercept from 1600 seconds into DOI

Note: All Group 3 cases are flown to rendezvous.

* P.A. Refers to Performance Analysis tests

** All Group 2 cases have radar schedules described in Section 6.2

Case 1.1 - Lunar Surface Landing

Description of Case and General Objectives

This case repeated the FP5 test case 1.1

The sequence of events comprising the test demonstrated the lunar landing operations and consisted of touchdown, store landing azimuth, self test reset, PGNCS to AGS attitude reference and state vector transfer, store landing azimuth following alignment and AGS off. The objective of the test was to verify that the AGS performed satisfactorily through all the above modes of operation and exhibited exact bit-by-bit agreement in regions unchanged by SCP's.

Conclusion

All the above operations were observed to occur as expected. A bit-by-bit comparison was made with the FP5 test results and exact agreement was observed for all quantities pertinent to the lunar surface operations. The telemetry output was checked and found to be correct.

Case 1.2 - Lunar Surface Abort

Description of Case and General Objectives

This case was initiated as a restart from Case 1.1 with appropriate modifications to simulate a lunar stay equivalent to a 3.5 deg azimuth rotation and a CSM/LM phasing at liftoff of 10.4 degrees which is equivalent to the phasing which exists when an abort occurs 656 seconds into the powered descent phase of the G Mission of Reference 8. The case began at 1040 sec with the LM on the lunar surface. Initially the computer start up routine was entered simulating the effects of turning the AGS on following shutdown. The AGS computer time was then initialized via the DEDA to test the computer time initialization routine. Then a PGNCS/AGS IMU alignment and a lunar surface gyro calibration were performed. New values of landing azimuth and the azimuth change during lunar stay were entered via the DEDA and control was switched to the AGS. The CSM and LM navigation data in the AGS computer were initialized by means of the DEDA and the AGS's DEDA initialize routine. The DEDA was then used to enter the orbit insertion targeting values. A body axis alignment was performed followed by a lunar alignment. After switching to automatic ($\beta_4 = 1$) and guidance steering ($S_{00} = 1$), an abort stage was commanded.

The thrust maneuver with the APS lasted from 1579.86 sec to 1990.52 sec. During the burn DEDA readouts of altitude, out-of-plane distance and velocity, and S_{11} were obtained. 100 sec from liftoff yaw steering to the $\underline{W}_b$ plane was begun and 50 sec later yaw steering was switched to the CSM orbit plane reference. New $\underline{W}_b$ components were entered and $\underline{W}_b$ yaw steering was resumed 250 seconds from liftoff. After APS cut-off, apofocus altitude and time to perifocus were read from the DEDA.

The objective of this case, in addition to demonstrating proper operation of the new orbit insertion logic following lunar surface abort, was to verify the proper operation of the lunar surface operations described above.

Conclusions

All the AGS computer operations tested in this case functioned correctly.

In addition to testing the AGS control of an APS orbit insertion maneuver burn from the lunar surface, this test case exercised the following AGS computer routines:

Start-up routine

Time initialization routine

PGNCS/AGS IMU alignment routine

Lunar surface gyro calibration routine

Lunar surface alignment routine

Body axis alignment routine

Yaw axis steering to both $\underline{W}_c$ and $\underline{W}_b$

LM and CSM DEDA initialization routines

Telemetry register loading in OI mode

Case 1.3 - CSI Burn with CDH 1/2 Orbital Period after CSI

The initial conditions for this case corresponded to those which exist at CSI time for the nominal G Mission of Reference 8. Preceding the CSI burn an in-flight accelerometer calibration, a downlink initialization, and an IMU alignment were performed and the targeting of the AGS computer for the desired line-of-sight angle was input via DEDA. Then control was transferred from the PGNCS to the AGS and the CSI burn performed using the RCS with the AGS in the External ΔV mode. After the completion of the burn, another accelerometer calibration was performed and several CSI and CDH guidance solutions targeted and observed via DEDA. The important quantities for each mode of operation as well as apofocus altitude and time to perifocus were read out both before and after the burn using the DEDA. Printout was obtained every minor cycle for two seconds to check the loading of the telemetry register in the CSI mode.

Conclusions

The in-flight accelerometer calibration errors were within quantization limits and all DEDA readouts were correct. The case demonstrated proper operation of the CSI routine using the half orbital period option, and showed similar characteristics as found in Case 1.14 and discussed in Section 2.1. The burn was correctly performed in the External ΔV mode. The telemetry register loading was correct.

Case 1.4 - CSI Burn with CDH 3/2 LM Orbital Period After CSI

Description of case and General Objectives

This case was initialized so that the LM and CSM states at the time of the CSI burn had the same perturbations as Case 6.11 of Reference 11. The perturbations are listed below for convenience.

	LM		CSM	
	Nominal	Perturbed	Nominal	Perturbed
Altitude(ft)	5885058	6100309	6066967	6066815
Velocity(ft/sec)	5396.06	5251.96	5342.87	5343.0
Flight Path ∢(deg)	89.9685	89.78	90.0	89.7

Phase ∢ CSM WRT LM $\theta c_{nom} = 9.85157^{\circ}$

$$\theta c_{perturbed} = 19.85^{\circ}$$

The objective of the case was to demonstrate the new CSI routine and an AGS controlled burn under perturbed conditions when the targeted CSI to CDH time was 3/2 LM orbital period.

Conclusions

This case demonstrated the proper operation of the CSI routine when the CDH maneuver is targeted to occur 3/2 LM orbital period after the CSI maneuver. The required burn was successfully targeted in the CSI mode and performed in the external ΔV mode.

This run satisfied the requirements of run number 4.7.3. of the LM/AGS P. and I. Specification.

Case 1.5 - CDH Burn Using External ΔV Pad Load

Case Description and General Objectives

This case was initialized with LM and CSM states identical to those used in FP5 test case 1.4. The burn was accomplished using the DPS.

LM vehicle perturbations of -10σ specific impulse, -10σ weight, and $+10\sigma$ thrust were used.

The simulated astronaut used the DEDA to target for a CDH burn using the external ΔV capability of the AGS. The ΔV components for the burn were those obtained from the similar FP5 case when the AGS was in the CDH mode. Printout was obtained every minor cycle for a 2 second interval to check the outputs of the telemetry register in the External ΔV mode.

Conclusions

This case demonstrated that the CDH burn may be executed by the AGS in the external ΔV mode using externally obtained ΔV components loaded by DEDA. The telemetry register was found to have the correct outputs and sequencing for the external ΔV mode.

This test satisfied the requirements of run number 4.7.3 of the LM/AGS P and I Specification.

Case 1.6 - CDH Burn with Removal of Out-of-CSM Plane Component of LM Velocity

Case Description and General Objectives

This test utilized the same initial states and sequence of astronaut events as FP5 test case 1.5. This consisted of a CDH burn utilizing the descent engine with the actual burn performed in the external ΔV mode, and LM vehicle perturbations of -10σ specific impulse, -10σ weight and -10σ thrust. Initially the LM orbit plane was at a wedge angle of .25 degrees from the CSM orbit plane and the LM position vector was along the line of nodes of these two planes. While in the CDH mode the simulated astronaut set the DEDA accessible quantity 28J2 equal to the AGS estimated value of the out-of-CSM plane velocity V_{py} prior to entering the External ΔV mode so as to demonstrate the use of the External ΔV mode in simultaneously performing the CDH burn and removing the out-of-CSM-plane component of the LM's velocity.

Conclusions

This case demonstrated that FP6 is capable of computing the CDH solution and simultaneously performing the CDH burn and removing the out-of-CSM-plane component of the LM's velocity. The telemetry values and sequencing for the CDH mode were verified to be correct. This test satisfied run number 4.7.3 of the LM/AGS P and I Specification.

Case 1.7 - TPI and First Midcourse Burn

Description of Case and General Objectives

This test was similar to the FP5 verification test case number 1.6 in initial states and sequence of astronaut instigated events. This corresponded to the LM above the CSM with a differential altitude of 107 nautical miles. Initially the LM orbital plane had a 0.6° wedge angle with the CSM orbital plane and the LM position was 45° from the node of the two planes. A time increment, J^4, was entered via DEDA so that the node of the LM/CSM orbital planes subsequent to the first TPI burn would be 82.1° from the LM's position at that time.

During the five minute period between TPI and midcourse all the meaningful AGS quantities accessible via DEDA were called for display. Numerous TPI guidance solutions were observed during the coast phase by entering various values of J^6 and J^4.

The objective of this case was to determine if the TPI guidance program in the AGS had remained essentially unchanged from that which existed for FP5.

This test satisfied run number 4.7.3. of the LM/AGS P. and I. Specification and the requirement imposed at the FP6 FACI that an ICS/FS case be performed where TPI execution is with the LM above the CSM.

Conclusions

It was concluded based on this test case that the TPI equations had been essentially unchanged from FP5 to FP6. The slight differences between the results of the two test cases were due to the following two sources.

(1) With the addition of the new radar filter in FP6, there is a delay in the time in the major 2-second cycle where the desired direction of the thrust axis ($\underline{X}_{bD}$) is updated. This gives a slightly different history of steering commands from the AGS to the autopilot.

(2) As part of TRW's policy of continuing to update, where feasible, the fidelity of the ICS/FS to the "real world", the "astronaut" model was updated for the FP6 verification testing so as to provide a more realistic simulation of the residual removal procedures following a main engine burn. This resulted in a slightly different (but more realistic) residual removal burn for the FP6 test case as compared with the FP5 test case. This slightly different burn at TPI resulted in slightly

different states at the time of the midcourse burn.

All quantities read out via the DEDA during the coast phase were verified to be correctly scaled and presented. Telemetry was also checked and found to be correct.

Case 1.8 - TPI Burn using Z-Axis RCS Engines and Z-Axis Steering

Case Description and Objectives

This case was similar to the FP5 test case 1.7. The constant J^4 was entered equal to zero such that a node at rendezvous was specified. The X-axis guidance steering and acquisition steering were each exercised prior to entering the Z-axis guidance steering mode used for the burn which utilized the 200 lb Z-axis RCS jets. During the coast phase of the run pertinent quantities were read out via the DEDA and various nodes other than at rendezvous were specified by having the simulated astronaut enter various values of J^4.

Conclusion

This case demonstrated that the TPI mode was programmed correctly. In addition it was verified that a Z-axis RCS burn can be performed using the external ΔV mode.

Case 1.9 - Abort from Hover

Description of Case and General Objectives

This case was initialized with LM conditions which exist when an abort is initiated late in the powered descent trajectory when the LM altitude is near 2000 feet. The primary objectives of the case were to test (1) the ability of the AGS to accept an altitude input to update the LM navigation data and (2) the new continuously variable orbit insertion targeting scheme where the LM orbit desired at insertion is a function of the relative geometry that exists between the LM and CSM prior to orbit insertion.

An abort stage was initiated after the altitude update and insertion was accomplished using the APS.

Conclusions

The case demonstrated (1) the AGS capability to update the estimated LM state from an altitude input and (2) the correct implementation of the continuously variable targeting scheme.

The APS was shut down at 59983 ft altitude and 19.2 fps altitude rate versus targets of 60,000 ft and 19.5 fps. The orbit insertion burn resulted in a 9.6 by 44.7 n.mi. coast orbit which is consistent with the LM to CSM phasing of this case.

Case 1.10 - Guidance Solutions During Coast

Description and Objectives

The case was initialized 456 seconds prior to CSI. Initial states were obtained from case 1.11 of the FP5 verification testing (which was initialized from an MSC G-mission reference trajectory). The test consisted of DEDA initialization of LM and CSM states, gyro and accelerometer calibration and examination of several guidance solutions. No burns were executed. The objectives of the case were (1) to examine gyro and accelerometer calibration convergence to proper compensation constants, (2) observe guidance solutions for proper operation, and (3) to demonstrate the ability to initialize the LM and CSM states via DEDA. CSI guidance solutions were attempted for TPI LOS angles of 15°, 26.6°, 30°, 45°, and 60°. In addition one CDH and one TPI solution were obtained. Guidance solutions were checked for overflows and proper reinitialization when switching between modes.

Conclusions

The LM and CSM initialization via DEDA was properly accomplished.

The ICS/FS guidance solutions compared favorably with those obtained from an engineering simulation. No improper overflows were observed. Guidance modes re-entered were correctly re-initialized.

The gyro bias compensation constants converged to within .03 deg/hr of a simulated bias of 1.00 deg/hr in each channel. The accelerometer compensation constants converged to within one half quantization level (12 µg) of a simulated bias of 300 µg in each channel. These errors are insignificant compared to the hardware bias instabilities.

Case 1.11 - Abort from Perturbed Descent Trajectory with the DPS at 50% Thrust

Case Description and General Objectives

This case simulated an abort with AGS takeover at t = 250 seconds into the powered descent phase of the G mission trajectory of Reference 8 with position and velocity perturbations of -14000 ft and -110 fps respectively in the radial direction and 15000 ft and 50 fps downrange and crossrange. These initial conditions and the sequence of events were similar to FP5 test case 1.12A. The orbit insertion was accomplished with the descent engine at 50% thrust, this level being maintained until completion of the maneuver.

The objectives of the case were, in general, to demonstrate the proper operation of the orbit insertion mode, and in particular to verify the proper operation of the continuously variable orbit insertion targeting (SCP 51).

Conclusions

Targeted pericynthion and apocynthion were observed to vary smoothly from 9.9 x 127.4 nmi near the start of the case to 9.9 x 111.3 at cutoff. The actual values after cutoff were 9.9 x 110.9. A minimum altitude of 7080 ft was reached at t = 336 sec when the altitude rate became positive. Vertical steering lasted until t = 354 sec. Engine cutoff occurred at t = 694.5 sec. Most of the equations used in the orbit insertion computations were checked by hand calculation.

The ICS/FS run was compared with its SFS counterpart. After adjusting for different thrust decay models, the ΔV expended compared within 0.5 fps and the apocynthion altitude within 0.5 nmi. It was not reasonable to compare this case with FP5 case 1.12A since different targeting criteria are used.

Case 1.12 - Abort Late in Powered Ascent

Case Description and General Objectives

This case was similar to FP5 test case 1.13 which began at 380 sec into the powered ascent phase of the G-mission of reference 8. The LM state has initial perturbations of 30000 ft and 40 fps from the nominal trajectory in each axis. This resulted in an initial out-of-CSM plane distance and velocity of -31385 ft and -19 fps (a wedge angle of .38° and an angle to the node of 125°). Initially the LM was at 97500 ft altitude in a staged situation under PGNCS control with the ascent engine on and a positive radial rate of 79.5 fps. At 382 seconds control of the APS engine and the vehicle's attitude control system was transferred to the AGS.

The objective of this case was to demonstrate AGS takeover during the ascent trajectory phase when large vehicle state perturbations from the nominal trajectory exist and to demonstrate the proper operation of the orbit insertion mode of the AGS with the newly programmed variable orbit insertion targeting (SCP No. 51). This case assumed that the lunar surface retargeting (8J and 9J) had not been performed. Printout was obtained every minor cycle for two seconds to check the loading of the telemetry register in the orbit insertion mode.

Conclusions

The AGS Orbit Insertion guidance controlled this abort from highly perturbed conditions late in powered ascent. The out-of-plane conditions for this case were not removed due to the small burn time remaining and the limiting of $\dddot{y}_d$. The wedge angle between LM and CSM orbit planes was reduced from 0.38 deg at abort to 0.31 deg at insertion, a time span of 26 sec. The AGS terminated thrust at 98800 ft altitude and 0.4 fps altitude rate demonstrating that the AGS does not steer to decrease excess altitude once it is achieved but does achieve velocity targets. The targets were 60000 ft altitude and 0 fps altitude rate. The 16.3 by 25.1 n.mi. orbit attained was acceptable in light of a target 16.2 by 24.8 n.mi. orbit as computed from θ_f.

Case 1.13 - Pre TPI Radar Filter Test

Description of Case and General Objective

This test case had the same initial LM and CSM states as test case 1.8 except that the LM navigation had extremely large errors introduced as follows.

Error	X-inertial	Y-inertial	Z-inertial
Position(feet)	30,000	6000	400,000
Velocity(feet/second)	300	20	40

Five radar range measurements were entered into the AGS at approximately 4 minute intervals. Between each radar range measurement and after the last range measurement two range rate measurements were taken at equally spaced intervals. All measurements were entered using the recommended operating procedure. No radar measurement noises, other than the quantization of range and range rate inputs, were simulated. During this test a multitude of CSI-CDH-TPI guidance solutions were made with switching from CSI to CDH to TPI and back and forth among these modes using the gamut of permissible targeting for each mode.

The primary objective of this test case was to demonstrate the capability of the AGS to accept radar data and properly process the same using the new radar filter. The secondary objective was to demonstrate the proper program operation in obtaining CSI, CDH, and TPI guidance solutions while taking radar data.

Conclusions

During this test a reduction in the navigation errors was observed following the radar range and range rate inputs. No unexpected overflow in any of the radar filter quantities were observed.

The CSI-CDH-TPI guidance solutions obtained during the periods between radar updates were compared with reference solutions obtained on an engineering simulation and good agreement was observed. The CSI-CDH solutions exibited the same discrepancy found in Case 1.14 and discussed in Section 2.1.

Case 1.14 - Pre CSI Radar Filter Test

Description of Case and General Objectives

This test case had the same initial conditions as test case 1.3 with the exception that the LM navigation had simulated errors as given below. These errors were made extremely large (up to 50σ) to stress the radar filter computations.

Error	x-inertial	y-inertial	z-inertial
Position (feet)	50,000	1000	500,000
Velocity (feet/second)	250	50	50

A series of radar range and range rate inputs via the DEDA were simulated. The range and range rates were obtained from a math model of the radar which had simulated noise added to the gimbal angles and the range rate.

The measurement schedule and noise for each reading is given below in terms of ellapsed time from the start of the case. In addition to the noise tabulated below, the range and range rate measurements were quantized at ±0.5 nmi and 0.1 fps, respectively.

Type Input	R	$\dot{R}$	R	$\dot{R}$	$\dot{R}$	$\dot{R}$	R	R	$\dot{R}$	$\dot{R}$
Time (sec)	10	100	190	280	370	460	550	670	730	790
Noise range rate (fps)		-0.1		-.5	.8	-.9			.6	-1.0
Noise Axis X-Gimbal (rad)	.005		-.002				.001	.004		
Noise Axis Y-Gimbal (rad)	-.001		.002				-.002	.007		

During this test the simulated flight crew targeted a multitude of CSI-CDH guidance solutions via the DEDA. (42 CSI and 5 CDH). Following the sequence of radar points a CSI burn was targeted and performed in the external ΔV mode. This run satisfied the LM/AGS P. and I. Specification run numbers 4.7.3. and 4.7.4.

The objective of this case was to demonstrate proper operation of the radar filter and other flight program computations simultaneously in the pre CSI condition. Extremely large LM state estimates and a non-nominal measurement schedule were used to stress the radar filter computations. Numerous non-nominal CSI and CDH targets were used to stress the guidance computations.

Conclusions

Proper simultaneous operation of the radar filter and other computations was observed. During this test a reduction in the navigation errors was observed following the radar range and range rate inputs. No unexpected overflow in any of the radar filter quantities were observed.

The CSI-CDH guidance solutions obtained during the periods between radar updates were compared with reference solutions obtained on an engineering simulation. This sequence of tests brought out the fact that if the magnitude of the velocity-to-be-gained in the CDH mode is desired for DEDA Readout, the External ΔV mode must be entered. The engineering simulation of the guidance equations was programmed to take this equation anomaly into account. Following this "correction" to the engineering simulation all AGS solutions were compared with the engineering simulation results and good agreement was observed. Section 2.1 contains a more detailed discussion of this anomaly.

The External ΔV routine was correctly targeted while the AGS was in the CSI mode so that when the External ΔV mode was entered the targeting was correct for performing the CSI burn.

6.2 Group 2 - Open Loop ICS Test Cases

6.2.1 Radar Filter Test Programs

The Interpretive Computer Simulation (ICS) and the Performance Analysis (PA) were the two programs used for the ICS open loop radar filter verification tests of the FP6 radar filter.

The ICS, being a bit-by-bit simulation of the flight computer, was suitable for the evaluation of the filter performance degradation due to numerical roundoff and truncation.

The PA was used to generate the required input quantities for the ICS. These quantities consisted of the scalar range and range rate radar data and the $\underline{Z}_b$ vector. The radar data were either noise-free or noisy. Each group of noisy radar data were generated by a single cycle Monte Carlo PA run. The measurement noise model is specified in Reference.

6.2.1.1 Summary of Test Areas

Four regions of the trajectory, Pre-CSI, Pre-CDH, Pre-TPI and Post TPI were utilized so that the effectiveness of the filter at all anticipated ranges could be studied. The Pre-CSI cases provided for evaluation of the long range performance of the filter and the combination of the four cases provided for evaluation of quantization and scaling adequacy.

The verification tests were designed to evaluate the following filter performance areas:

1) demonstrate that the filter equations are coded correctly in the AEA;
2) filter accuracy degradation due to FP6 computer word length limitation;
3) adequacy of scalings and quantizations used for all quantities in the filter;
4) demonstrate equivalence of the filter implementations in the PA and ICS programs.

The demonstration of PA-ICS filter equivalency was an important step as the PA Monte Carlo runs were used to evaluate the statistical performance of the FP6 lunar rendezvous capability.

6.2.1.2 ICS Filter Test Cases

Cases 2.1 - 2.4 3σ Radar Filter Test Cases (Schedule 1)

In all 3σ test runs, the initial x and z positions were perturbed by 30,000 ft., y position by 45,000 ft., and the initial x and z velocities by 30 fps., the y velocity by 45 fps.

Measurement Schedule 1

R	$\dot{R}$	$\dot{R}$	R	$\dot{R}$	$\dot{R}$	R	$\dot{R}$	$\dot{R}$	R	$\dot{R}$	$\dot{R}$	R	$\dot{R}$	$\dot{R}$
240	320	400	480	560	640	720	800	880	960	1040	1120	1200	1280	1360

Radar measurement schedule 1 consists of five range radar measurements each followed by two range rate measurements, containing a total of 15 radar measurements. For a given maximum radar time span and other maneuver constraints, this schedule had yielded favorable results in previous single-case noisy performance analysis simulations. A total of 16 test runs were made. The first 8 cases were run with the noise-free measurement data, the remaining 8 cases were run with noise contaminated measurement data. These tests were created mainly to check the coding adequacy of the ICS FP6 radar filter and to study the magnitude of the quantization errors. It should be emphasized that the actual radar filter performance evaluation should be done by means of the Monte Carlo performance analysis simulations. The test results discussed in this document bear no significance in determining the filter performance since the noise-free runs were not realistic cases and the cases with noise were an insufficient sample for suitable filter performance evaluation.

Cases 2.5 - 2.8 3σ Radar Filter Test Cases (Schedule 2)

Measurement Schedule 2

	R	R	R	$\dot{R}$	$\dot{R}$	R	R	R
0	120	240	360	400	440	480	600	720

This schedule consists of 6 range measurements and 2 range rate measurement after the third range point. 8 cases with radar measurement noise and another 8 without measurement noise were run. The test specified in this section would provide additional results to show that the FP6 radar filter properly operated under different measurement schedules, noisy data and initial condition errors. Special emphasis in these tests were given to observing if underflows or overflows occurred in any of the radar filter equations.

Case 2.9 - 2.12 <u>3σ Radar Filter Test Cases</u> (Schedule 3)

Measurement Schedule 3

0	400	480	560	640	720	800	880	960	1200
	R	$\dot{R}$	$\dot{R}$	$\dot{R}$	$\dot{R}$	R	$\dot{R}$	$\dot{R}$	R

A total of 16 noise-free and noisy radar measurement cases were run for this schedule to provide additional results.

Cases 2.13 - 2.16 <u>Nominal Radar Filter Test Cases</u> (Schedule 1 and 4)

Measurement Schedule 4

0	256	384	512	516	640	704	768	848	928	1040
	R	$\dot{R}$	R	$\dot{R}$	$\dot{R}$	$\dot{R}$	R	$\dot{R}$	$\dot{R}$	R

In these test cases, the initial conditions of the LM were not perturbed. A total of 40 cases were run these included the following special measurement conditions.

1) no radar taken
2) no measurement noise
3) R noise only
4) $\dot{R}$ noise only
5) $\underline{Z}_b$ noise only
6) R, $\dot{R}$, and $\underline{Z}_b$ noise

Case 2.17 - 2.20 <u>10σ Radar Filter Test Cases</u> (Schedules 1 and 4)

For these test cases, the LM initial inplane positions were perturbed by 100,000 ft., inplane velocities by 100 fps., out-of-plane position by 150,000 ft. and out-of-plane velocity by 150 fps.

These extremely large initial state perturbations were not realistic. They were designed to provide additional verification of correctness of filter coding and to test for possible overflows and underflows. The measurement conditions were the same as in Cases 2.12-2.15.

6.2.1.3 Summary of Test Results

(1) No unexplained overflows or underflows occurred in any of the test cases.

(2) In all test cases, estimated state errors converged with additional processed radar data, showing that the filter has performed properly.

(3) When a sufficient number of noise-free radar data had been processed, the maximum position and velocity roundoff errors over the nominal trajectory were found to be below 1,700 ft and 1.6 fps respectively. The roundoff errors were slightly higher when the filter was in the transient state. The ICS numerical roundoff was reflected in the filter weight deviations from those obtained from the PA program as shown in Figs. 6.2.1.3(a).

(4) When the ICS states, filter weights and covariance matrices, were compared point by point with the corresponding PA quantities, no unexplained discrepancies resulted in any of the test cases. After all radar data had been processed, the deviations between the ICS and PA states were small. These discrepancies were usually smaller than the final ICS estimated state errors.

6.2.1.4 Conclusions

(1) The ICS radar filter tests that were performed indicated no coding or scaling errors.

(2) Detailed comparison of the many PA and ICS test cases demonstrated the equivalence of the radar filter implementations in the PA and ICS programs.

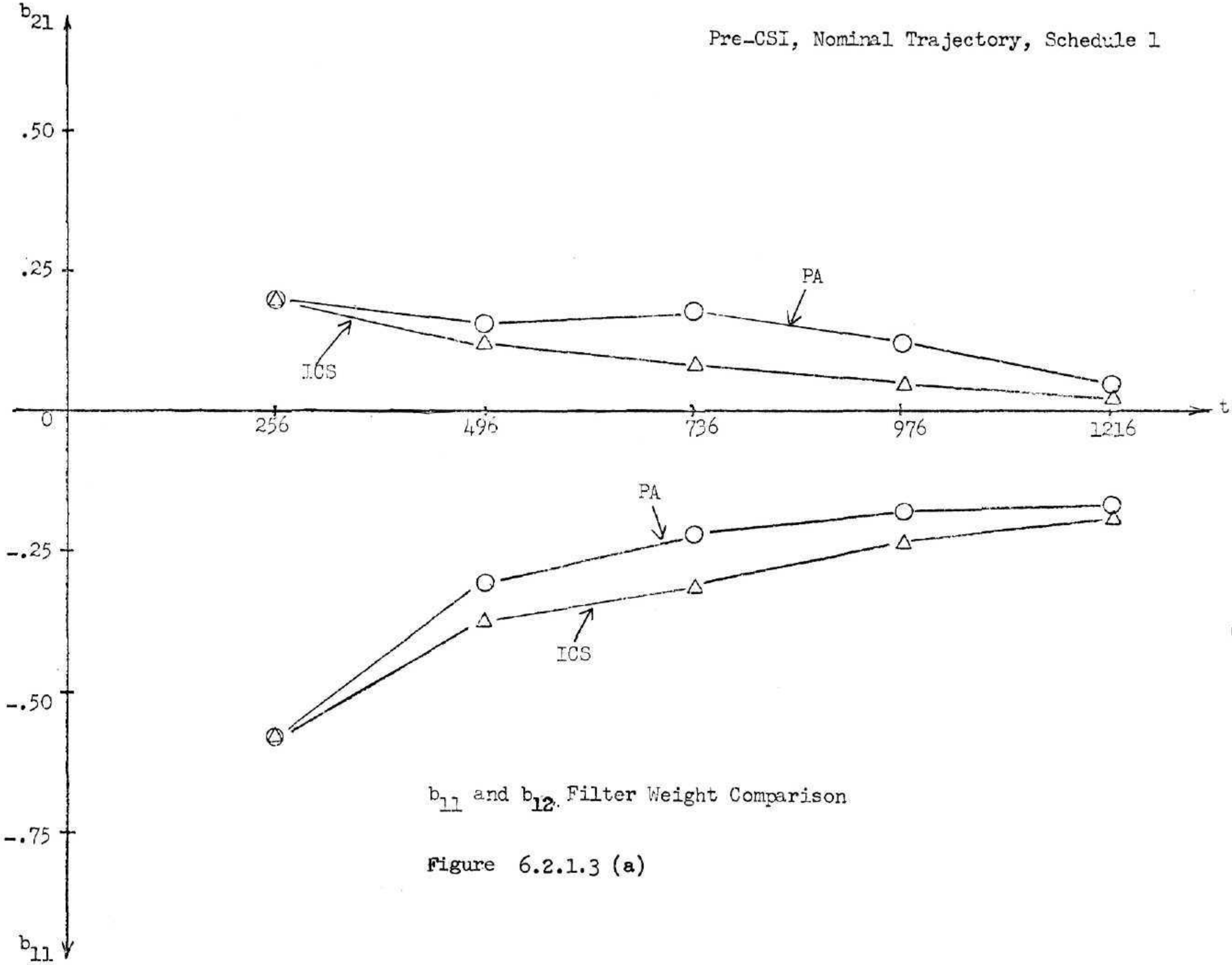

b_{11} and b_{12} Filter Weight Comparison

Figure 6.2.1.3 (a)

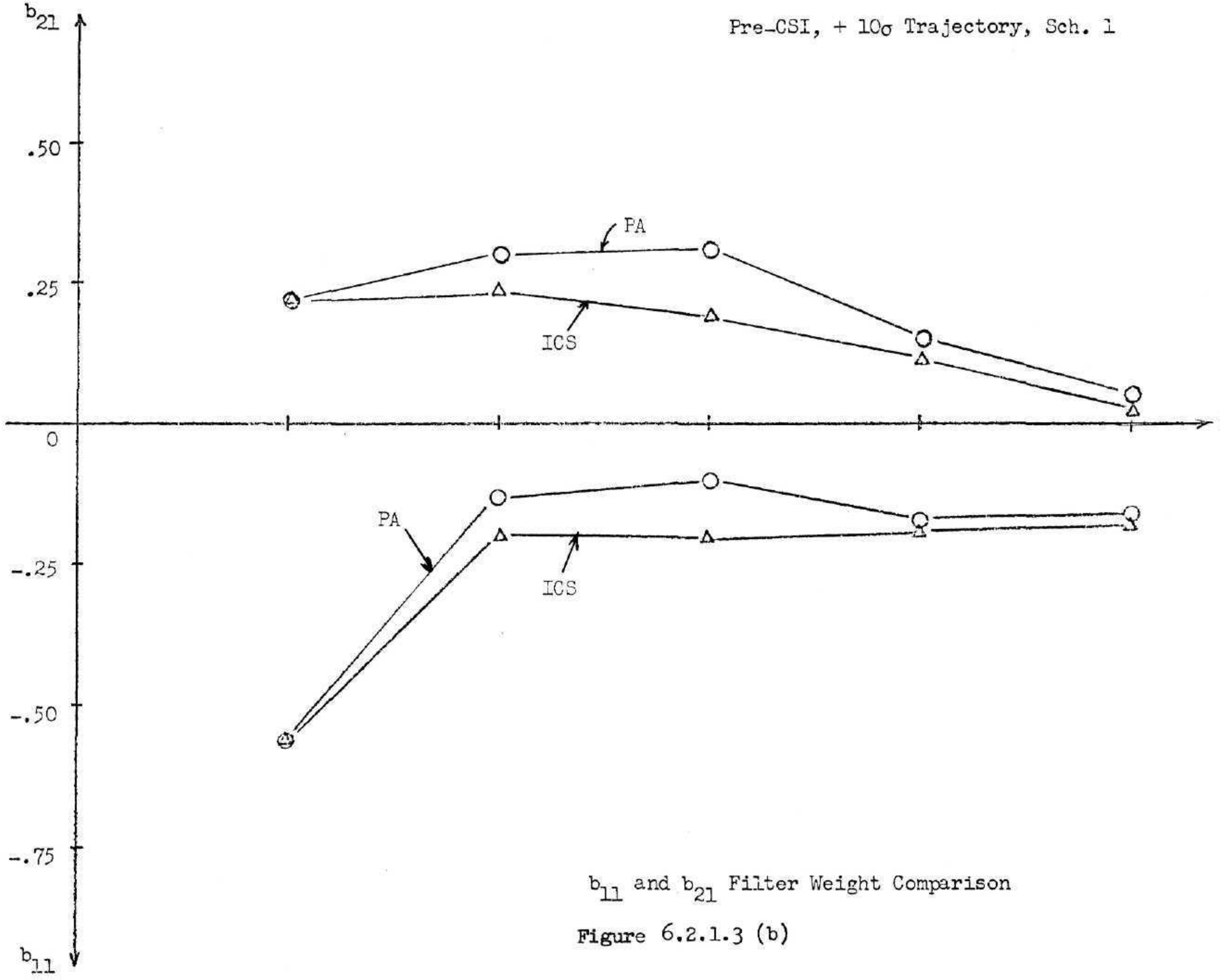

b_{11} and b_{21} Filter Weight Comparison

Figure 6.2.1.3 (b)

6.2.2 CSI and CDH Open Loop Test Cases

Description of Cases and General Objectives

A series of 23 CSI cases and 6 CDH cases consisting of highly perturbed vehicle states and target conditions were run in an open loop manner in the ICS. The CSI case perturbations consisted of the following conditions at CSI:

LM altitude	±200,000 ft
LM velocity	±100 fps
LM altitude rate	±94 fps
LM state 55 min. after OI for abort at PDI	
CSM Orbit	55 x 65 n.mi.
LM to CSM central angle	-10 deg and +30 deg
Target TPI time	nominal ±20 min
Target TPI time	270 min after CSI
Target Elevation Angle	-16.6 deg and 71.6 deg
3/2 Orbital Period CSI to CDH time with perturbations.	
Several cases with combined perturbations.	

The CDH case perturbations consisted of the following conditions which were selected from the CSI cases.

Δh in coelliptic orbit	-16 n.mi. and +65 n.mi.
LM altitude rate at CDH	±90 fps
LM to CSM Central Angle at CSI	-10 deg and +30 deg

These perturbations which in many cases are unrealistically large were selected to test FP6 for possible problems in the CSI and CDH routines. They also provided data on the accuracy of FP6 CSI and CDH solutions in light of quantization errors.

Conclusions

The results of these ICS tests were compared to the results of identical scientific tests. The resulting difference represents the affect of AEA quantization and round off errors in the CSI or CDH routines. Then differences do not include initialization errors, algorithm errors or navigation errors.

The CSI solution was within 0.5 fps of the scientific solution for CSI ΔV and predicted CDH ΔV. Predicted Δh was within 0.1 n.mi.

The CDH solution was within 0.3 fps of the scientific solution for CDH ΔV. The Δh solution was within 0.14 n.mi.

These errors are small and therefore acceptable in light of the FP6 radar filter performance. The radar filter will be used to update vehicle states prior to CSI.

6.3 Group 3 - SFS Test Case Results

The SFS duplicated the Group 1 ICS/FS cases with the exception of Case 1.1, which is a lunar surface case. Guidance solutions, maneuver parameters, fuel consumption, and other parameters were cross-checked for consistency.

Group 3 consisted of SFS cases starting at various abort points in the G Mission and running through the rendezvous sequence. The main test objectives for group 3 included, a) verification of the variable orbit insertion targeting equations for the entire range of aborts during the powered descent phase and b) evaluation of the FP6 CSI-CDH equation performance for complete rendezvous sequences from the entire range of possible post, orbit insertion trajectories.

6.3.1 Summary of Group 3 Results

The detailed results of the group 3 cases are presented in Table 6.2. In summary, the equation performance was shown to be acceptable and no problems were encountered in the test cases. The CSI-CDH equations operated within their anticipated accuracies and the orbit insertion targeting performed correctly during powered descent aborts.

Table 6.2 - Scientific Simulation Test Results

Case	Description	Insertion Orbit	Post CSI Orbit	Post CDH Orbit (1)	CSM Orbit	ΔV O.I.	ΔV CSI	ΔV CDH	ΔV TPI	Braking ΔV	Post-CDH Δr (N.M.)	J^1	Actual TPI Time ($\theta_{LOS} = 26.6^o$)
3.1	Lunar surface abort with LM initially 2 deg out of CSM orbit plane	9.0 x 45.9	44.8 x 45.7	44.8 x 45.7	60.0 x 60.6	6060.8	50.4	0.0	143.5(2)	36.4	15.0	9172	9162
3.3	Abort prior to CSI with +20000 ft and +10 ft/sec LM out-of-plane perturbations	10.2 x 45.9	44.5 x 45.9	43.9 x 44.4	59.9 x 60.7	-	109.4(3)	2.8	36.5	34.6	16.1	9172	8890(3)
3.4	Same as 3.3 except perturbations were -20000 ft and -10 ft/sec	9.8 x 45.9	44.5 x 45.9	43.9 x 44.5	59.9 x 60.7	-	109.8(3)	3.0	35.8	34.3	16.1	9172	8898(3)
3.5	Abort at PDI +100 sec with 100% DPS throttle	9.4 x 135.0	31.7 x 135.7	38.0 x 42.0	59.2 x 60.2	1109.3	31.8	203.9	38.8	39.6	17.4(4)	9460	9510
3.5	Abort at PDI +100 sec with 50% DPS throttle	9.8 x 134.2	33.1 x 136.1	40.1 x 42.8	59.7 x 60.1	988.4	32.3	201.6	37.0	37.9	16.7	9540	9592
3.6	Abort at PDI +200 sec with 100% DPS throttle	9.8 x 127.3	32.6 x 127.3	38.2 x 41.9	59.7 x 60.1	2351.6	32.7	185.1	37.8	39.3	17.8	9358	9366
3.7	Abort at PDI +350 sec with 100% DPS throttle	10.2 x 101.6	36.0 x 102.2	39.7 x 42.0	59.8 x 60.1	4343.2	36.7	127.5	33.8	38.0	18.5	9140	9266
3.8	Abort at PDI +500 sec with 100% DPS throttle	11.7 x 61.0	37.6 x 61.2	38.6 x 39.2	57.9 x 58.8	5767.8	36.4	44.6	33.4	41.9	19.4	8950	8950
3.9	Abort stage at hover	9.3 x 31.2	30.6 x 34.3	33.8 x 34.6	57.9 x 58.8	6028.4	34.9	4.6	40.0	51.0	24.3(5)	8829	8872
3.10	Nominal surface abort under AGS control	9.0 x 46.0	45.2 x 46.0	45.2 x 45.8	60.0 x 60.6	6037.3	50.8	0.8	24.2	32.8	14.9	9176	9189
3.13	Abort at PDI +150 sec with positive P&I Spec perturbations and 100% DPS	15.2 x 126.5	34.9 x 127.6	42.1 x 44.3	59.7 x 60.1	1658.2	28.6	178.5	50.0	32.5	15.4	9376	9406
3.14	Same as 3.3 except with negative P&I Spec perturbations	7.6 x 131.7	31.9 x 133.8	39.4 x 41.7	59.7 x 60.1	2201.1	36.2	196.0	35.7	54.3	18.3	9416	9850
3.15	Surface abort with APS premature shutdown at 404 sec, RCS takeover to insertion	9.4 x 44.7	-	-	-	6035.5	-	-	-	-	-	-	-
3.16	Abort at DOI +1600 sec, direct transfer back to CSM	-	-	-	58.0 x 59.0	-	-	-	253.4	83.2	-	-	-

(1) All orbit dimensions are the actual dynamics values. In most cases the guidance estimate of the post CDH orbit indicated an orbit more coelliptic to the CSM orbit (±1 nmi). Navigation errors contribute to this difference.

(2) The insertion maneuver resulted in a 1 1/2 deg wedge angle between the LM and CSM orbit planes at insertion, as expected. The TPI maneuver must remove considerable out-of-plane velocity to achieve the correct transfer, which gives a larger TPI ΔV than in the nominal (in-plane) surface abort case 3.10.

(3) The CSI maneuver removed all out-of-plane velocity ~ 98 ft/sec. This results in introducing errors into the CSI maneuver that result in obtaining the desired line-of-sight prior to the nominal TPI time. This same phenomenon, observed and analyzed in FP5 verification results, is due to the fact that the CSI ΔV solution does not include the 28J2 component. Consequently, when the 28J2 component is added to the CSI ΔV the magnitude of the resulting post CSI LM velocity is smaller than that computed by the CSI routine. The post CSI orbit thus has a fast catch-up rate and will achieve the desired line-of-sight sooner.

(4) The orbit insertion variable targeting constants that control the post CDH Δr were not "tuned" to achieve a specific Δr for all abort situations

(5) The LM-CSM phasing at abort from hover is such that the nominal rendezvous time line results in the orbits as shown. TRW understands that in order to raise the post CDH Δr to 15 nmi an External ΔV at nominal CSI is added to the sequence and the remaining rendezvous maneuvers are slipped 1/2 orbit.

Appendix A

Flight Program Changes Since FP5

Table A-1 is a list of the software changes used to generate LM/AGS FP6-S03A from FP5 and the ICS/FS verification test cases which check each change

Table 1

Software Change No.	Description	Verification Cases
43	Expanded Capability Radar Filter	1.13, 1.14
50	Addition of CSI/CDH Equations to Flight Programs Containing the Expanded Capability Radar Filter	1.3, 1.4, 1.5, 1.6, 1.10, 1.13, 1.14
51	Provide Equations in the Flight Program which Continuously Update the Desired Orbit Insertion Conditions	1.2, 1.9, 1.11, 1.12

References

(1) 11176-6035-T000, "Program Verification Test Plan - LM/AGS Flight Program X," dated January 1969.

(2) TRW Report No. 11176-6041-TOOO, "LM/AGS Programmed Equations Document, Flight Program 6," dated April 1969.

(3) MSC document (no number), "Minutes, LM/AGS Flight Program X (FPX) First Article Configuration Inspection (FACI)", dated February 24-25, 1969.

(4) TRW Report No. 11176-6042-TOOO, "LM/AGS Computer Program Specification, Flight Program 6," by G.H. Friedman, dated March 1969.

(5) TRW Report No. 11176-6029-TOOO, "Program Verification Test Results, LM/AGS Flight Program 5," by E.V. Avery, dated January 1969.

(6) TRW Report No. 05952-6211-T000, "Program Verification Test Results, LM/AGS Flight Program 3," by R.L. Eshbaugh, dated May 1968.

(7) TRW Report No. 05952-6142-TOOO, "LM/AGS Program Verification Test Results, Design Mission Computer Program," Revision B, Vol. 1 and 2, by R.L. Eshbaugh, K.L. Baker and H.V. Kienberger, dated April 1967.

(8) MSC Listing - G Mission Trajectory Listing, dated 17 February 1969 (provided at FPX FACI).

(9) TRW Report No. 05952-6157-T000, "DMCP LM AGS Interpretive Computer Simulation/Flight Simulation (ICS/FS) Description," dated March 1968.

(10) TRW Report No. 11176-6033-TOOO, "LM/AGS Operating Manual FP6," by R.L. Mendelsberg, dated April 1969.

(11) TRW Report No. 11176-6024-TOOO, "FPX CSI/CDH Equations Including Test Results," by R.L. Eshbaugh, dated December 1968.